

Context-Aware Fail-Safe Multi-Modal Sensor Fusion Framework for Autonomous Vehicle Navigation in an Indoor Environment

Muhammad Asim Rehmat¹, Hammad Hassan^{1,2*},
Muhammad Ahmad Hassan^{1,2}, Mirza Haseeb Khalid¹,
Hafiz Muhammad Ali⁵, Muhammad Haroon Yousaf Khalid⁴,
Haider Abbas³

¹Department of Computer Engineering, UET, Lahore, Pakistan.

²Al-Khawarizmi Institute Of Computer Science, UET, Lahore, Pakistan.

³National University of Sciences & Technology, Islamabad, Pakistan.

⁴Department of Computer Engineering, UET, Taxila, Taxila, Pakistan.

⁵King Fahad University of Petroleum and Minerals, , Saudia Arabia.

*Corresponding author(s). E-mail(s): hammad.hassan@kics.edu.pk;

Contributing authors: asimrehmat@uet.edu.pk;

ahmed.hasan@kics.edu.pk; enr.mhaseebk@gmail.com;

hafiz.ali@kfupm.edu.sa; haroon.yousaf@uettaxila.edu.pk;

haiderabbas-mcs@nust.edu.pk;

Abstract

Indoor autonomous vehicles face persistent localization challenges due to sensor failures, path restrictions, illumination changes, and dynamic obstacles. We propose a fail-safe, context-aware, multi-modal sensor fusion framework to ensure reliable navigation. The approach combines ensemble localization, confidence-weighted fusion via Kalman consensus, and a fail-safe decision algorithm integrated with adaptive path planning. Sensor weights are dynamically adjusted to maintain accuracy under partial or complete modality failures. We used the "Haram" (pilgrimage ritual (Tawaf)) as an inspirational application for the simulation and evaluation of the proposed framework. For this purpose, we created an AV cart and replicated it by maintaining the challenges of an interior setting, a comparable path length, and occlusions. The work covers the equivalent environmental applicability to other complex environments such as airports, hospitals, and shopping malls. The framework is implemented in ROS

with a 3D-customized cart navigating circular and elliptical paths under simulated sensor networks. Performance evaluation using Average Displacement Error (ADE), Final Displacement Error (FDE), collisions, and trip completion time shows improved robustness and higher success rates than static fusion, even under repeated sensor failure scenarios.

Keywords: Autonomous Vehicle, Fail-Safe Systems, Heterogeneous Sensor Networks, Kalman Filter, Robotic Operating System (ROS), Source Localization, Robot Operating System (ROS)

1 Introduction

Autonomous mobile robots are increasingly being explored as intelligent assistants for navigation and mobility in crowded indoor environments. A prime example is the dense crowd during the Islamic Tawaf ritual in Makkah, where millions of pilgrims congregate in a limited area. During peak periods, the pilgrim density can reach extreme levels – around 150,000 people performing Tawaf per hour, with local densities up to about 8 individuals per square meter near the Kaaba. Such intense crowding often exceeds the available space and poses severe challenges for conventional mobility aids. While manual wheelchairs and electric mobility scooters (carrying at most two people) have been introduced to assist elderly and disabled pilgrims, these solutions are limited by the need for human operators and dedicated lanes. Moreover, physical expansion of the holy site is constrained by religious and structural factors, so simply adding more space or more manual helpers is not feasible. These constraints motivate the development of an autonomous robotic navigation system that can safely operate in such dense crowds, improving mobility assistance without additional infrastructure.

Navigating an autonomous vehicle through a heterogeneous, high-density crowd like the Tawaf scenario is an exceedingly complex robotics problem. The crowd's behavior is non-uniform: individuals move with different speeds and intentions – some steadily circumambulating, others stopping suddenly or moving orthogonally to the main flow to approach or exit the area. Flow patterns continuously form and dissipate, and proximity to the Kaaba or local obstacles causes variable movement speeds. This results in dynamic streams of people with frequent unpredictable changes, making collision avoidance and path planning difficult. Furthermore, the indoor setting and dense human body occlusions mean that traditional navigation sensors face reliability issues. For example, GPS is unavailable indoors, visual sensors can be obstructed or suffer in low-light conditions, and even LiDAR rangefinders may be affected by reflections or by people blocking the line of sight. Wireless signals used for localization (e.g. WiFi or Bluetooth beacons) become erratic under crowd-induced multipath interference and attenuation. These challenges demand a navigation framework that is not only accurate in tracking the robot's position and planning paths, but also resilient to sensor failures, occlusions, and environmental changes.

To meet these challenges, we propose a context-aware, fail-safe multi-modal sensor fusion framework for autonomous indoor navigation. The robotic platform is equipped

with a heterogeneous suite of sensors – including LiDAR, cameras, Bluetooth Low Energy (BLE) beacons, WiFi receivers, infrared (IR) proximity sensors, and RFID tags – providing complementary perspectives of the environment. Each modality contributes unique strengths: LiDAR and cameras offer rich spatial perception for obstacle detection and mapping, wireless BLE/WiFi signals and RFID tags provide additional localization cues in GPS-denied settings, and IR sensors plus wheel odometry supply short-range distance and motion feedback. By fusing these diverse inputs, the system builds a robust understanding of its environment that remains operative even if certain sensors become unreliable. Crucially, our framework is context-aware – it continually assesses the quality of each sensor stream and the environmental conditions, and then prioritizes or re-weights sensor inputs accordingly. For instance, if the camera’s view is compromised by poor lighting or occlusion, the algorithm increases reliance on LiDAR and radio-frequency based measurements; conversely, if wireless signal readings (RSSI) are unstable due to interference, vision and LiDAR data are given greater weight. This adaptive sensor fusion strategy ensures fail-safe redundancy: the robot’s localization and perception remain accurate and drift-free even in the presence of individual sensor degradation or failure. In essence, no single point of sensor failure will incapacitate the navigation system – it can “gracefully degrade” by falling back on alternate sensing modalities as needed.

Another key aspect of our approach is an integrated adaptive path planning and fail-safe control mechanism. The autonomous vehicle not only fuses sensor data for localization, but also adjusts its navigation strategy based on the current context and confidence in the sensor inputs. A fail-safe decision module monitors for abnormal conditions such as sensor drop-outs or detections of exceptionally crowded or dark areas. When such conditions are identified, the system triggers appropriate mitigation behaviors in real time. For example, the robot may slow down, take an alternative route, or switch to a more conservative navigation mode if its awareness of the environment diminishes. This close coupling between the sensor-fusion module and the motion planner allows the robot to continuously maintain safe operation despite the dynamic, unpredictable nature of the crowd. In other words, redundancy handling and resilient localization are complemented by on-line adaptive planning – together forming a fail-safe control loop that prioritizes safety and reliability in all circumstances. This framework builds upon concepts like ensemble localization and confidence-weighted Kalman filtering, combined with a high-level decision layer that enforces safe navigation policies when uncertainties arise.

We have implemented the proposed multi-modal fusion and navigation system on a prototype robotic cart using the Robot Operating System (ROS) platform. To evaluate its performance, we developed a 3D simulation of the Tawaf environment, in which a virtual autonomous cart navigates along representative circular and elliptical paths among simulated crowds and sensor input. The use of ROS allowed for seamless integration of the various sensor data streams and control algorithms in real time. We evaluated the system’s localization accuracy and navigation reliability under a range of challenging scenarios, including cases where sensors intermittently fail or produce corrupted data. Key performance metrics such as Average Displacement Error (ADE), Final Displacement Error (FDE), collision count, and trip completion time

were recorded. The results demonstrate that our context-aware fusion framework substantially improves robustness and success rates compared to a static sensor fusion baseline. Even when subject to repeated sensor failures, the autonomous cart was able to maintain accurate location and successfully complete its route with minimal collisions, while a nonadaptive approach often became lost or unsafe. These findings validate the effectiveness of incorporating adaptive, fail-safe sensor fusion and planning for indoor autonomous navigation. Furthermore, although our case study centers on the extreme conditions of the Makkah pilgrimage, the principles and system architecture are broadly applicable to similar dynamic indoor environments such as airports, transit stations, shopping malls, hospitals, and industrial sites. In all these settings, an autonomous robot must deal with moving crowds, occlusions, and sensor uncertainties. Our work contributes to a generalizable framework for robust multisensor indoor navigation that can enhance safety and reliability in such complex and crowded environments.

2 Related Work

Autonomous navigation in crowded indoor environments, such as pilgrimage rituals such as Tawaf in Makkah, poses formidable challenges that involve dense human movement, occlusions, and limited access to external localization [1, 2]. Simulations of such extreme crowd densities highlight how conventional path planning fails under emergent crowd dynamics. Recent systems employing LiDAR-based detection and tracking, such as [3], have demonstrated improved obstacle avoidance in moving crowds, yet reliable crowd-aware robotic navigation remains elusive.

To achieve robust localization under such conditions, multi-modal sensor fusion has emerged as a crucial strategy. EKF-based frameworks that fuse sensors like vision, IMU, ultra-sonic, WiFi, and BLE deliver more stable state estimates than single-modal systems. [4] propose a two-stage EKF-based positioning system that seamlessly switches between ultrasonic-IMU fusion and visual ArUco tracking when visibility degrades. Similarly, [5] employ a two-stage EKF correction by using accelerometer and compass data for accurate indoor location of an ambulance robot, demonstrating practical applicability to service robotics in constrained environments.

They [6] enhances Monte Carlo Localization to combat illumination changes, dynamic environments, and kidnapping issues—further ensuring robust mapping and positioning in indoor navigation tasks. Authors in [7] propose a bio-inspired hybrid path planning that integrates ACO, WOA, APF, and random jumps for efficient, collision-free navigation in dynamic environments, underscoring the necessity for adaptable trajectory generation that accounts for real-time sensor uncertainties. Robust indoor localization in GPS-denied environments often relies on multi-sensor fusion. For example, they [8] fused UWB, odometry, and AHRS using a Kalman filter to significantly reduce noise and drift. Similarly, authors in [9] combined EKF with recurrent neural networks (RNNs) to achieve localization accuracy within 8 cm, outperforming traditional SLAM baselines. They [10] proposed a resilient factor-graph fusion of LiDAR, IMU, and UWB for quadruped robots, enabling robust positioning even under non-line-of-sight radio conditions.

Crowd-aware navigation introduces additional challenges. Authors in [11] addressed navigation among moving obstacles with a dynamics-aware NMPC controller, achieving safer high-speed navigation in dense scenarios. The authors of the work of comparison of classical and deep-reinforcement-learning-based planners of indoor mobile robots in dynamic crowds [12] emphasize the domains in which the methods of learning prevail over traditional techniques. Moreover, reliable autonomous functions require to be fail-safe and fault-tolerant. In the article by [13], the authors have shown decentralized fault-tolerant formation control of a multi-robot team with LiDAR faults that resolved sensor redundancy and inter-robot validation. Likewise, the authors of the article [14] have introduced an IMM-based multiple-model Kalman filter, which is capable of identifying and isolating faulty sensors in real time to allow robust navigation under the negatively sensing conditions.

Also, Robotic algorithm development greatly benefits from simulation platforms that offer modularity, repeatability, and real-time testing before deployment. The Robot Operating System (ROS) has emerged as a leading middleware for such purposes due to its hardware abstraction, standardized communication protocols, and extensive ecosystem of packages and tools [15, 16]. For example, Gazebo remains one of the most widely used simulators for Industry 4.0/5.0-related robotics due to seamless integration with ROS and ROS 2 [17]. Studies comparing ROS-compatible simulators show that while Ignition and Webots offer greater stability, frameworks such as CoppeliaSim and PyBullet are more resource-efficient, highlighting ROS's flexibility in accommodating diverse simulation requirements [16].

ROS also accelerates development through simulation-in-the-loop prototyping, allowing developers to test perception, planning, and control algorithms rapidly across multiple simulated environments before deploying on physical robots [15]. Middleware communication through ROS topics, services, and actions enables interchangeable sensor and actuator models, which streamlines integration and supports advanced simulation workflows such as digital twins and multi-robot coordination [15]. ROS 2 further enhances this capability by introducing improvements in real-time performance, security, and multi-platform support, making it suitable for modern robotics scenarios that demand dependable simulation infrastructure [18].

Together, these works illustrate the rapid progress in multi-sensor fusion, crowd-aware planning, and fault-tolerant design, yet also highlight the need for a unified framework that integrates these capabilities for robust operation in highly dense indoor environments.

Additionally, autonomous robot navigation in complex domains such as radiation-affected uneven terrain employs multi-layer costmaps and sensor fusion-based real-time localization and control, as seen in [19]. Nonetheless, key gaps persist. Most existing systems focus on nominal operation and single-point sensor redundancy, with limited logic for detecting and responding to sensor faults in real time. Few architectures enable **graceful degradation**, where navigation behavior dynamically adjusts (e.g., re-routes, slowdowns) in proportion to sensor confidence drops. In addition, the interaction between adaptive sensor confidence assessment, fail-safe decision making, and motion planning remains underdeveloped, especially in human-dense contexts such as Tawaf.

In response, our work proposes a unified framework that integrates multi-modal sensor fusion (LiDAR, camera, BLE, IR, WiFi, odometry), adaptive confidence weighting, and fail-safe planning. Implemented in ROS and evaluated under Tawaf-like simulation, it seeks to close the gap by enabling robust, autonomous navigation among dense crowds, with explicit redundancy handling, sensor health monitoring, and context-aware motion control.

3 Proposed Architecture

The proposed framework ensures robust localization by fusing complementary sensors. LiDAR and camera provide fine-grained local positioning, BLE and IR improve short-range accuracy, and WiFi acts as a global fallback. Dynamic covariance adjustment enables prioritization of reliable sensors under varying conditions. We have put forth an intelligent model for ritual completion. Our design enables the simultaneous movement of multiple carts providing a capacity of four humans provided per cart. The objectives covered mainly, has been listed as follows,

- Driving capacity of 4 people per cart.
- Self-Control
- Navigation and collision avoidance
- Path Following mechanism
- Multi-modal sensors and network infrastructure.
- Cart to Cart Cart to global network-based localization framework
- Event-based movement and direction control.
- Pilgrims interactive device for verses/recitation.
- Emergency control and mechanism.
- Multi-level localization to provide foolproof fail-safe drive.

In this work, we designed a multi-sensor fusion framework for an indoor autonomous cart. The framework fuses odometry, LiDAR, camera, BLE, IR, and WiFi signals using an Extended Kalman Filter (EKF) to provide robust localization even under degraded sensing conditions. The system model has been explained as follows,

A layer of heterogeneous sensing layers with redundancy is maintained to allow the vehicle to be securely driven in independent mode. The primary components of our suggested remedy are as follows:

- Cart Registration Process
- Cart Navigation by performing localization, ensuring the safety and criticality measures.
- Communication for real-time monitoring and needs-based for human intervention.

The proposed architecture, illustrated in Figure 1, is composed of the following core modules: a *Sensors Layer*, a *Context Inference Module*, a *Sensor Confidence Estimator*, an *Adaptive Fusion Core*, and a *Fail-Safe Controller*. The workflow begins with the public CART registration process, followed by the navigation module, which governs motion planning and control.

The *Sensors Layer* is divided into two primary components:

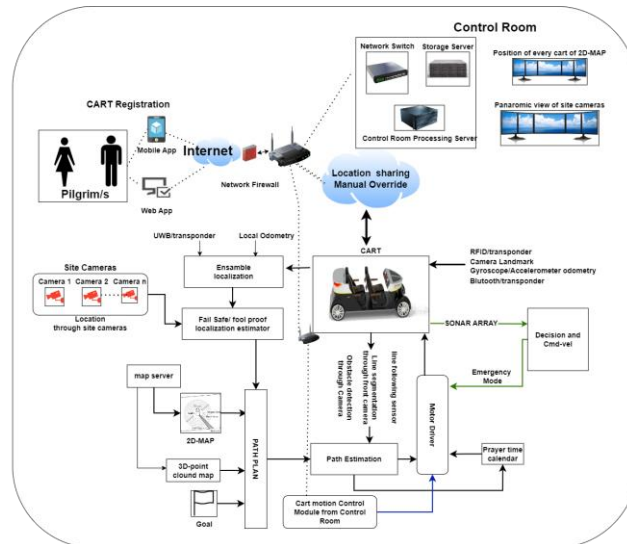


Fig. 1: Proposed Architecture and Components

1. **Localization and Path Estimation:** achieved through the fusion of multiple sensors, odometry, and path estimation data.
2. **Cart Motion and Control System:** responsible for dynamic actuation and trajectory execution based on localization feedback.

4 Proposed Methodology

4.1 System State and Motion Model

The system state is defined by the cart's 2D position and orientation. Using wheel encoder data, forward displacement is estimated from the average of left and right wheel motions, while orientation change is derived from their difference relative to the wheelbase. The updated state is then computed through the odometry motion model, with process noise covariance Q accounting for uncertainty.

The system state is represented by the vector

$$\mathbf{x}_t = [x_t \ y_t \ \vartheta_t]^T, \quad (1)$$

where (x_t, y_t) is the 2D position and ϑ_t is the orientation of the cart.

Using wheel encoder readings from the right and left $\Delta S_R, \Delta S_L$, wheels, the odometry-based motion model is derived. The average wheel displacement gives the forward motion: Given wheel encoder readings, the odometry-based motion model is:

$$\Delta S = \frac{\Delta S_R + \Delta S_L}{2}, \quad (2)$$

$$\Delta \vartheta = \frac{\Delta S_R - \Delta S_L}{b}, \quad (3)$$

$$\mathbf{x}_{t|t-1} = \begin{bmatrix} x_{t-1} + \Delta s \cos(\vartheta_{t-1} + \frac{\Delta\vartheta}{2}) \\ y_{t-1} + \Delta s \sin(\vartheta_{t-1} + \frac{\Delta\vartheta}{2}) \\ \vartheta_{t-1} + \Delta\vartheta \end{bmatrix}, \quad (4)$$

where b is the wheelbase. The motion uncertainty is modeled by process noise covariance Q .

4.2 Sensor Models

Each sensor provides a measurement z with an associated noise covariance R , enabling multi-modal sensor fusion for robust localization. The considered sensor models are:

- **LiDAR:**

$$z_{lidar} = h_{lidar}(\mathbf{x}_t, M) + v_{lidar}, \quad (5)$$

where M is the map. LiDAR enables scan-matching for accurate localization but is sensitive to occlusion and reflective surfaces.

- **Camera (Visual Odometry):**

$$z_{vo} = h_{vo}(\mathbf{x}_t) + v_{vo}, \quad (6)$$

providing motion estimates from image sequences. Performance degrades in low-light or textureless environments.

- **BLE (Bluetooth Low Energy):**

$$z_{ble} = h_{ble}(\mathbf{x}_t) + v_{ble}, \quad (7)$$

enabling beacon-based ranging. It offers coarse localization but suffers from multi-path effects and interference.

- **IR (Infrared Proximity):**

$$z_{ir} = h_{ir}(\mathbf{x}_t) + v_{ir}, \quad (8)$$

suitable for short-range obstacle detection, though limited in range.

- **WiFi (Fallback):**

$$z_{wifi} = h_{wifi}(\mathbf{x}_t) + v_{wifi}, \quad (9)$$

providing coarse global localization from signal strength. Used as a fallback when higher-precision sensors degrade.

4.3 Extended Kalman Filter

The prediction step:

$$\mathbf{x}_{t|t-1} = f(\mathbf{x}_{t-1}, u_t) + w_t, \quad (10)$$

$$P_{t|t-1} = F_t P_{t-1} F_t^T + Q_t, \quad (11)$$

where F_t is the Jacobian of f and w_t is process noise.

The update step for each sensor measurement (z, R):

$$y = z - h(\mathbf{x}_{t|t-1}), \quad (12)$$

$$S = HP_{t|t-1}H^T + R, \quad (13)$$

$$K = P_{t|t-1}H^T S^{-1}, \quad (14)$$

$$\mathbf{x}_{t|t} = \mathbf{x}_{t|t-1} + Ky, \quad (15)$$

$$P_{t|t} = (I - KH)P_{t|t-1}, \quad (16)$$

where H is the Jacobian of h .

4.4 Sensor Prioritization

Dynamic re-weighting is applied:

$$R' = \alpha R, \quad \alpha \geq 1, \quad (17)$$

where α increases if sensor confidence is low (e.g., poor lighting for the camera, multipath interference for BLE, or high noise in WiFi).

4.4.1 Map-Aided Correction

A 2D occupancy grid map M is maintained using LiDAR scans:

$$M_t = \text{InverseSensorUpdate}(M_{t-1}, z_{\text{lidar}}, \hat{\mathbf{x}}_{t|t}), \quad (18)$$

where the function updates occupancy probabilities based on the current LiDAR scan and estimated pose.

For localization correction, LiDAR scan matching (e.g., ICP or NDT) provides a measurement of the cart's position relative to the map:

$$z_{\text{map}} = h_{\text{map}}(\mathbf{x}_t, M) + v_{\text{map}}, \quad (19)$$

which is fused into the EKF update step with covariance R_{map} .

4.4.2 Combined Localization Framework

Thus, the final localization framework integrates:

- High-frequency **odometry** updates (short-term consistency).
- **Map-based corrections** using LiDAR scan matching (long-term accuracy).
- Additional sensor updates (camera, BLE, IR, WiFi) for robustness in challenging conditions.

4.5 Sensor Prioritization and Fusion

The combined localization framework merges high-rate odometry with LiDAR-based map corrections to achieve robust, drift-free positioning. High-frequency odometry

(wheel encoder dead reckoning) provides continuous short-term pose updates but accumulates drift over time. To counteract this drift, the framework periodically performs LiDAR scan matching against a known map, eliminating accumulated error and preserving long-term accuracy.

In parallel, an Extended Kalman Filter (EKF) fuses additional modalities – including camera visual odometry, BLE beacon ranging, infrared (IR) proximity sensing, and WiFi signal measurements – as supplementary observations. These heterogeneous sensor inputs provide fail-safe redundancy and context-aware corrections under challenging conditions (e.g., poor lighting affecting cameras or multipath interference degrading wireless signals). By dynamically integrating all sources, the system maintains real-time responsiveness and precise pose estimation. This multi-modal approach ensures resilient indoor localization that remains accurate and drift-free even in the presence of individual sensor degradation or failure.

- Increase R_{cam} in poor lighting.
- Increase R_{lidar} in reflective environments.
- Increase R_{ble} if RSSI is unstable.
- Increase R_{wifi} (always lower confidence).

Fusion is performed via EKF update:

$$K_t = P_{t|t-1} H_t^T (H_t P_{t|t-1} H_t^T + R_t)^{-1}, \quad (20)$$

$$\mathbf{x}_{t|t} = \mathbf{x}_{t|t-1} + K_t (z_t - h(\mathbf{x}_{t|t-1})), \quad (21)$$

$$P_{t|t} = (I - K_t H_t) P_{t|t-1}. \quad (22)$$

4.6 Unified Algorithm

Algorithm 1 Multi-Sensor Fusion with Map and Odometry

```

1: Initialize  $\mathbf{x}_0, P_0, M_0$ 
2: while robot is running do
3:   Prediction: Update  $\mathbf{x}_{t|t-1}, P_{t|t-1}$  using odometry
4:   Collect data: LiDAR, Camera, BLE, IR, WiFi
5:   if LiDAR available then
6:     Perform scan matching, update  $M_t$ , compute  $z_{map}$ 
7:   end if
8:   for all measurements  $z_i$  do
9:     Adjust covariance  $R_i$  according to environment (prioritization)
10:    if measurement passes consistency check then
11:      EKF update with  $z_i, R_i$ 
12:    end if
13:  end for
14:  Publish  $\mathbf{x}_{t|t}, P_{t|t}$ 
15: end while

```

4.7 Cart Design and Sensors Integration

The implementation of the processing of data from a heterogeneous sensor layer as well as the methods of localization through state estimation are used to achieve navigation. In our model the following layer of sensors is kept as local to cart to ensure the fail-safe autonomous operations.

- RFID Transponders
- Gyroscope / Accelerometer odometry
- Bluetooth / Transponder
- Line Following Sensor

The sensor placement can be visualized in Figure 2. The RFID tags serve as transponders for cart localization and carry profile information such as speed and motion-related data. In parallel, an onboard accelerometer is employed to capture vibrations generated by the motor during transitions from rest to motion, thereby providing an additional modality for detecting and characterizing dynamic cart behavior.



Fig. 2: Hetrogeneous Sensor Array: Left to Right; 1- Stereo Vision Camera, 2- RFID Transponders, 3- Bluetooth / Transponder , 4- Line Following Sensor Array

Two fisheye cameras are mounted on the front of the cart to enable stereo vision, which supports tracking, obstacle avoidance, and object identification through the stereo video feed. In addition to vision, a Bluetooth transponder provides two distinct functions: inter-cart communication and localization. The transponder has been installed at the base of the cart, while Bluetooth beacons are deployed in both stationary and movable regions of the environment. Each device is assigned a unique identifier; when a cart carrying a matching ID enters the range of a beacon, the system recognizes the cart and retrieves its corresponding position data.

For line-following capabilities, an array of five infrared (IR) sensors is mounted beneath the cart. These sensors operate by emitting IR light and measuring the

reflected intensity to detect the presence and curvature of the line, enabling precise path tracking along predefined routes.

The exact CART design has been shown in figures 3 and 4.



Fig. 3: Design view of Electric Cart Vehicle



Fig. 4: Abstract view of Electric Cart Vehicle and Sensors

The detailed specifications and details of the components for the particular cart have been listed in tables 1 and 2.

5 Experiment and Results

The experimental setup has been simulated in Robot Operating System (ROS) with a maze consisting of a round path in the surroundings of elliptical path as of KABA in Haram, as shown in figures 5 and 6.

The path is created as shown in figure 7 similar to physical existence of Haram (Place of Rituals).

We employed the Intel RealSense T265 tracking camera, which provides 3-axis visual-inertial odometry supported by an integrated accelerometer and gyroscope. The corresponding ROS node extracts odometry data via the serial interface for real-time navigation. To evaluate robustness under varying sensor conditions, we defined a

S.No	Item Name	Specifications
1	Body	Fiberglass Body with Metallic Chassis
2	Length	2330 mm (2 Seater), 3033 mm (4 Seater)
3	Width	1488 mm
4	Height	1380 mm
5	Max Curb Weight	275 kg (2 Seater), 325 Kg
6	Min Turn Radius	3.2 meters
7	Gr. Clearance	100 mm
8	Tyres	175/55R15

Table 1: Specifications

S.No	Item Name	Specifications
1	Electric Motor	80V,4KW
2	Battery	82V, 75AH (Quick Replacement)
3	Controller	Vector Control
4	Charger	80V/25A (3 hours Charging Time)
5	Max Speed	15 km/h (Adjustable on Authorization)
6	Max Range	80 KM
7	Brake and Range	Front and Rear and <5 m
8	Steering	Rack & Pinion, Electronic Power

Table 2: The detail of the components



Fig. 5: Simulation Path: Side view

sequence of simulation iterations with different sensor availability scenarios, including complete failure and no-failure cases. The complete set of iterations is summarized in Table 3. At the last iteration where we considered the failure of all sensors, a manual driver mode has been enabled.

In this regard, the results are gathered in the form of Average Displacement Error (ADE), Final Displacement Error (FDE), No of Collision and Trip completion time. Figure 8 shows the estimation and selection of the route even in the presence of the shortest route algorithm.

The error matrices for determining the trajectory path accuracy have been gathered in the form of ADE and FDE. The subsequent results for ADE and FDE are shown in figure 9 and 10. Average Displacement Error (ADE): ADE refers to the mean square error (MSE) over all estimated points of every trajectory and the true points. The respective results for ADE are gathered in the presence of no of occlusions and with change in no of carts.

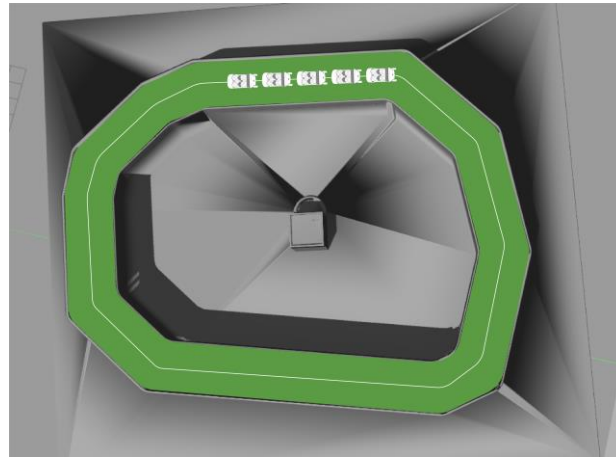


Fig. 6: Simulation Path:TOP view



Fig. 7: Haram: Actual Location

whereas the metric of FDE has been captured to find the distance between the predicted final destination and the true final destination at the $T_{P\ period}$ time. The respective results for FDE are gathered in presence of no of occlusions and with change in no of carts.

Similarly, a metric showing no of collisions during the cart movements provided there are iteration of occlusions along with the change in no of cart. The respective results has been shown in figure 11.

The measurement is no only kept to precise performance metrics as defined above but along with these, the time to complete the trip has been recorded to measure the time performance during the simulation. The results are normalized into range of 0 to 1. 1 tends to infinity which defines and infinite time i.e the fail safe over mode in which

Iteration #	Sensor Failure	Failover Alternate
1	None	All Sensors
2	LIDAR	Camera, BLE
3	LIDAR, Camera	BLE, IR
4	LIDAR, Camera, BLE	IR, RSSI, Map Odometry
5	LIDAR, Camer, BLE, IR RSSI	CCTV
6	All Sensor	Manual Mode

Table 3: Sensor Failure vs Failover

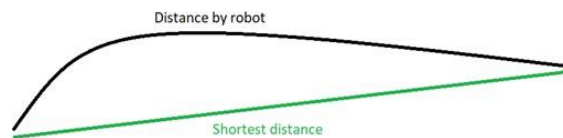


Fig. 8: Path Estimation

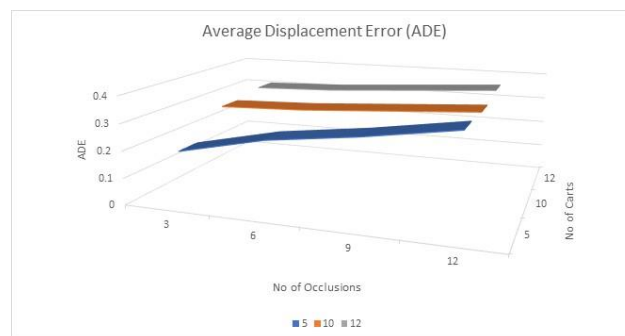


Fig. 9: Average Displacement Error with multiple Carts and Occlusions in Between

all sensing has been disabled and the system is safely stopped through manual override mode. The subsequent result for the time parameter has been shown in figure 12.

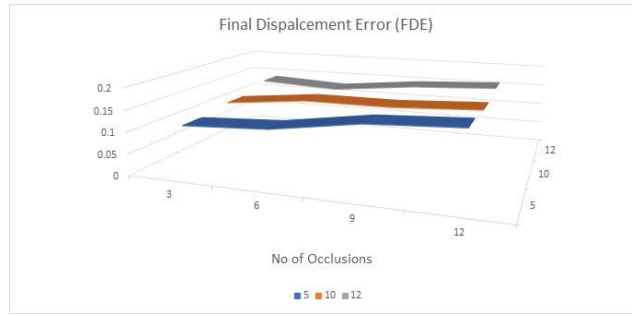


Fig. 10: Final Displacement Error with multiple Carts and Occlusions in Between

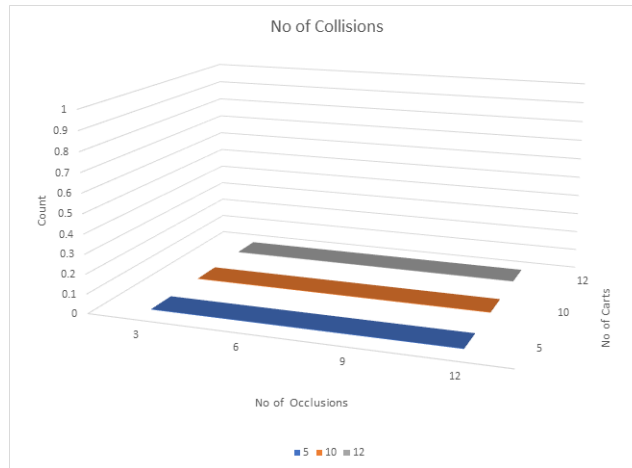


Fig. 11: No of Collision with obstacle / Occlusions

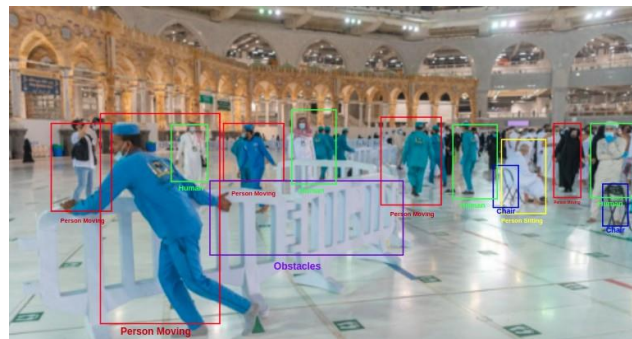


Fig. 13: Sample Results of Object/s Detection

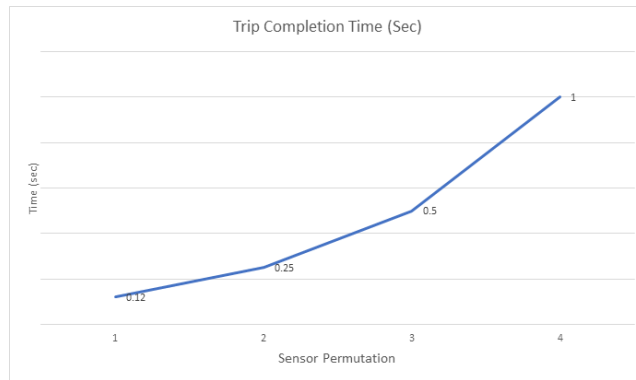


Fig. 12: Trip Completion Time

The output results of this module is shown in figure 13. We assign a unique ID to every CART to make their tracking easy.

6 Conclusion

This work has been carried out to devise the complete design of autonomous cart with capacity of carrying four people simultaneously for performing rituals at a specific location in Haram. The design has been presented with edge processing, localization with heterogeneous sensor data fusion and network data management. The proposed design ensures the operations around real-time localization, autonomous mode for operation, safety and criticality measures, object detection, monitoring and vehicle management system. We employed path estimation techniques, source localization, sensor and fail-over mechanism. For this purpose, the complete solution has been simulated in Robot Operating System (ROS). The results for quality, real-time processing and parametric evaluation are presented notifying the displacement error, no of collisions and route deviations for single or multi-cart scenarios. Additionally this is just the case study and the developed solution can be generalized for all such applications required inside the malls, airports, amusement parks, shipping yards, ware houses and specifically in manufacturing lines where human and robots needs to work together.

7 Funding Declaration

This research did not receive a specific grant from any funding agency in the public, commercial or non-profit sectors.

References

- [1] Curtis, S., Guy, S.J., Zafar, B., Manocha, D.: Virtual tawaf: A case study in simulating the behavior of dense, heterogeneous crowds, 128–135 (2011). IEEE

- [2] Kurdi, O., Stannett, M., Romano, D.M.: Modeling and simulation of tawaf and sa'yee: A survey of recent work in the field (2015)
- [3] Xu, J., Zhang, W., Cai, J., Liu, H.: Safecrowdnav: Safety evaluation of robot crowd navigation in complex scenes. *Frontiers in Neurorobotics* **17**, 1276519 (2023) <https://doi.org/10.3389/fnbot.2023.1276519>
- [4] Yang, X., Yang, Y.: Two-stage multi-sensor fusion positioning system with seamless switching. *International Journal of Intelligent Robotics and Applications* **7**(3), 345–357 (2023) <https://doi.org/10.1007/s41315-023-00276-0>
- [5] Yang, C.Y., Zhang, H., Li, M., Liu, W.: Two-stage extended kalman filter correction for accurate localization of an ambulance robot. *International Journal of Intelligent Robotics and Applications* **8**(2), 123–136 (2024) <https://doi.org/10.1007/s41315-024-00352-z>
- [6] Agunbiade, O.Y.: Enhancing the mcl-slam algorithm to overcome the issue of illumination variation, non-static environment and kidnapping to present the nik-slam. *International Journal of Intelligent Robotics and Applications* (2024) <https://doi.org/10.1007/s41315-024-00396-1> . online first
- [7] Yuan, L., Chen, J., Wu, Y.: A bio-inspired hybrid path planning algorithm for dynamic environments. *International Journal of Intelligent Robotics and Applications* **9**(1), 79–94 (2025) <https://doi.org/10.1007/s41315-025-00479-7>
- [8] Tran, Q.-K., Ryoo, Y.-J.: Multi-sensor fusion framework for reliable localization and trajectory tracking of mobile robot by integrating uwb, odometry, and ahrs. *Biomimetics* **10**(7), 478 (2025)
- [9] Huang, Z., Ye, G., Yang, P., Yu, W.: Application of multi-sensor fusion localization algorithm based on recurrent neural networks. *Scientific Reports* **15**(8195) (2025)
- [10] Kuang, Y., Hu, T., Ouyang, M., Yang, Y., Zhang, X.: Tightly coupled lidar/imu/uwb fusion via resilient factor graph for quadruped robot positioning. *Remote Sensing* **16**(22), 4171 (2024)
- [11] Tarantos, S.G., Belvedere, T., Oriolo, G.: Dynamics-aware navigation among moving obstacles with application to ground and flying robots. *Robotics and Autonomous Systems* **172**, 104582 (2024)
- [12] Arce, D., Solano, J., Beltrán, C.: A comparison study between traditional and deep-reinforcement-learning-based algorithms for indoor autonomous navigation in dynamic scenarios. *Sensors* **23**(24), 9672 (2023)
- [13] Elsayed, A.M., Elshalakani, M., Hammad, S.A., Maged, S.A.: Decentralized fault-tolerant control of multi-mobile robot system addressing lidar sensor faults.

Scientific Reports **14**(25713) (2024)

- [14] Kheirandish, M., Azadi Yazdi, E., Mohammadi, H.: A fault-tolerant sensor fusion in mobile robots using multiple model kalman filters. *Robotics and Autonomous Systems* **161**, 104324 (2023)
- [15] Aljamal, M.: Comprehensive review of robotics operating system [ros] in simulation and prototyping contexts. *Applied Sciences* **15**(4), 1840 (2025)
- [16] Audonnet, F.P., Hamilton, A., Aragon-Camarasa, G.: A systematic comparison of simulation software for robotic arm manipulation using ros2. arXiv preprint arXiv:2204.06433 (2022). preprint
- [17] Flores Gonzalez, J.M., Coronado, E., Yamanobe, N.: Ros-compatible robotics simulators for industry 4.0 and industry 5.0: A systematic review of trends and technologies. *Applied Sciences* **15**(15), 8637 (2025) <https://doi.org/10.3390/app15158637>
- [18] Macenski, S., Foote, T., Gerkey, B., Lalancette, C., Woodall, W.: Robot operating system 2: Design, architecture, and uses in the wild. arXiv preprint arXiv:2211.07752 (2022). preprint
- [19] Huang, Z., Li, P., Zhao, Y.: Autonomous robot navigation in radiation-affected uneven terrain using multi-layer costmaps. *International Journal of Intelligent Robotics and Applications* **6**(4), 327–342 (2022) <https://doi.org/10.1007/s41315-022-00255-x>